AJNR

A Comparison of Magnetization Transfer Ratio, Magnetization Transfer Rate, and the Native Relaxation Time of Water Protons Related to Relapsing-remitting Multiple Sclerosis

Stefan Ropele, Siegried Strasser-Fuchs, Michael Augustin, Rudolf Stollberger, Christian Enzinger, Hans-Peter Hartung and Franz Fazekas

AJNR Am J Neuroradiol 2000, 21 (10) 1885-1891
http://www.ajnr.org/content/21/10/1885

AJNR Am J Neuroradiol 21:1885–1891, November/December 2000

A Comparison of Magnetization Transfer Ratio, Magnetization Transfer Rate, and the Native Relaxation Time of Water Protons Related to Relapsing-remitting Multiple Sclerosis

Stefan Ropele, Siegried Strasser-Fuchs, Michael Augustin, Rudolf Stollberger, Christian Enzinger, Hans-Peter Hartung, and Franz Fazekas

BACKGROUND AND PURPOSE: **Magnetization transfer (MT) imaging and measurements of the magnetization transfer ratio (MTR) have extended our capability to depict and characterize pathologic changes associated with multiple sclerosis (MS). We wanted to investigate whether the analysis of other MT parameters, such as magnetization transfer rate (k_{for}) and relative measure of water content ($T1_{free}$), adds insight into MS-related tissue changes.**

METHODS: **Quantitative MT imaging by use of phase acquisition of composite echoes was performed in nine patients with clinically definite relapsing-remitting MS and eight healthy control subjects on a 1.5-T MR system. We analyzed a total of 360 regions of interest and compared control white matter with various types of lesions and normal-appearing white matter in MS.**

RESULTS: **We found a strong correlation between the MTR and k_{for}, but this relation was non-linear. A slight but significant reduction of the MTR in normal-appearing white matter of patients with MS was attributable to a reduced transfer rate only, whereas a lower MTR was associated with both a reduction of k_{for} and an increase of $T1_{free}$ in regions of dirty white matter. Moreover, areas such as edema and T1-isointense lesions had a similar MTR but could be differentiated on the basis of $T1_{free}$.**

CONCLUSION: **Estimates of k_{for} and $T1_{free}$ appear to complement MTR measurements for the understanding of MT changes that occur with different types of MS abnormalities in the brain.**

MR imaging has become an important tool to aid in diagnosing multiple sclerosis (MS) and to obtain objective outcome measures regarding activity and progression of this disease in clinical trials (1, 2). The ability of conventional MR sequences to show the histopathologic heterogeneity of MS lesions is, however, insufficient. This prohibits a closer look at the evolution of MS-related tissue changes and is considered a main reason for limited correlations between clinical disability and lesion extent as shown by routine MR (2, 3). Magnetization transfer (MT) imaging holds great promise for improving this situation, because it allows some distinction between protons associated with macromolecules and those contained in free water (4). In MS, shifts between these proton pools can be caused both by edema and a variety of structural changes (5). Importantly, MT imaging is especially sensitive for damage to myelinated fibers, because myelin is considered a main source for the pool of protons bound to macromulecules (6, 7). Hence, numerous contributions have recently explored the potential of MT imaging for better lesion characterization (8, 9) and for improving clinicoradiologic correlations in MS (10, 11).

Quantitation of MT in these studies usually has been based on calculations of the magnetization transfer ratio (MTR). This is a relative measure of the reduction in signal intensity due to the MT effect and a complex function of many processes in-

Received January 2, 2000; accepted after revision May 23.

From the Department of Neurology (S.R., S.S-F., M.A., C.E., H-P.H. F.F.), Magnetic Resonance Institute (S.R., R.S., F.F.), Karl-Franzens University of Graz, Austria.

This work was supported in part by grants of the European Charcot Foundation (Nijmegen, The Netherlands) and the Gemeinnützige Hertie Stiftung (Frankfurt, Germany), grant GHS-319/94. Prof. Klaus V. Toyka, Dept. of Neurology, Julius-Maximilian University, Würzburg, Germany is thanked for support of the study.

Address reprint requests to Franz Fazekas, MD, Department of Neurology, Karl-Franzens University, Auenbruggerplatz 22, A-8036 Graz, Austria.

volved in spin-lattice relaxation and cross relaxation (12). Therefore, further insight into the mechanisms of MTR reduction described with MS-related tissue changes should be expected from the analysis of individual variables contributing to the MTR. Under the condition of fully selective saturation of macromolecular protons, the MTR could be viewed as a function of the magnetization transfer rate (k_{for}) and the native relaxation time of the water protons ($T1_{free}$) (13). Although this condition may not be achievable in vivo, an estimation of these variables would appear to be a first step toward multiparametric analysis. Such estimation of MTR, k_{for}, and $T1_{free}$ can now be achieved with a new sequence called *fast phase acquisition of composite echoes* (FastPACE) (14–16).

Methods

Quantitative MT Technique

Immobile water protons, which are bound to macromolecules such as the myelin lipids or proteins, cannot be detected by conventional MR imaging owing to their extremely short T2 relaxation time (<1 ms) (17). However, through dipole-dipole coupling and chemical exchange, these protons exchange magnetization with ''MR-visible'' protons associated to the ''free'' mobile bulk water. When the protons of the bound pool are selectively saturated by using spectral selective RF pulses, saturated magnetization is subsequently transferred to the free pool. This results in a decrease of steady-state magnetization (18). Currently this effect has been measured by calculating the MTR by the equation MTR = 1—M_S/M_0, where M_0 is the steady-state magnetization in the absence of saturation and M_s is the magnetization in the presence of saturation; ie, MTR images reflect the difference of two scans obtained with and without prior energy saturation of macromolecular protons.

Generally, the MTR is a function of several fundamental parameters of each pool. In the ideal case where the myelin pool is almost completely saturated, MTR becomes a function of just a few fundamental parameters (13). One possible view then is to consider the MTR as: $MTR = k_{for} \cdot T1_{free}/(1+ k_{for} \cdot T1_{free})$. In this equation, k_{for} is a constant that gives the first-order magnetization transfer rate. $T1_{free}$ is the native longitudinal relaxation time of the free mobile water pool in the absence of MT. $T1_{free}$ is a function of the macromolecular concentration and independent of the amount of MT (19). Therefore, it can serve as a relative measure for the water content.

The equation cited in the previous paragraph was initially derived by Forsen and Hoffman to study chemical exchange (20), and, in the strict sense, can be applied only if one pool of protons is fully saturated while the other remains unaffected. In vivo experiments may not completely fulfill this prerequisite because of RF pulse power limitations due to tissue heating and overlapping resonance frequencies of both spin species (21). Therefore, in vivo measures of MTR, k_{for}, and $T1_{free}$ have to be considered as estimates depending on experimental settings rather than absolute quantities. However, recent results from numerical simulations performed for white matter (22) indicate that a very high saturation level can be achieved also on a clinical scanner with acceptable RF pulse power.

We recently have developed a method that allows for simultaneous acquisition of MTR, k_{for}, and $T1_{free}$(14, 15). This FastPACE sequence is a two-point T1 mapping method, which encodes T1 in the phase of an MR image. The corresponding pulse diagram is depicted in Figure 1. An essential feature of this sequence is the symmetrical application of the RF pulses, which allows for multislice T1 mapping during efficient, pulsed MT saturation. Therefore, FastPACE provides a reliable multislice parameter estimation within a clinically reasonable acquisition time of about 10 minutes.

Subjects

This study was conducted in nine patients with clinically definite MS who were selected consecutively from the outpatient department of our clinic because of recent clinical deterioration. They were six women and three men ranging in age from 25 to 50 years (mean age, 38 years). All patients suffered from a relapsing-remitting course and had an Expanded Disability Status Scale (EDSS) score (23) ranging from 1.0 to 5.0. Five of these patients were on long-term immunomodulatory treatment. Eight healthy volunteers (four women and four men, 18 to 45 years old) with no previous history of neurologic disease served as control subjects. The protocol was approved by our institutional review board, and written consent was obtained from all patients and volunteers.

MR Imaging

Conventional MR imaging and quantitative MT imaging were performed on a 1.5-T unit (Gyroscan ACS-NT; Philips, The Netherlands) using the standard head coil. Head motion was minimized with foam pads. The scanning protocol was consistently as follows:

1. Localizing scan in axial, sagittal, and coronal planes.
2. FastPACE sequence, as shown in Figure 1, (580/20 [TR/TE], $\alpha_1 = 45°$, phase cycling = 90°/0°, number of averages = 2) with and without an MT saturation pulse (1–2–1 binomial, on-resonant pulse with a duration of 1 ms and a peak amplitude of 23.6 μT)
3. Precontrast T1-weighted conventional spin echo (CSE) (510/14 [TR/TE], number of averages = 2)
4. Dual-echo CSE (2060/20–80 TR/TE)
5. Postcontrast T1-weighted CSE (510/14 [TR/TE], number of averages = 2) obtained 5 minutes after IV application of 0.1 mmol/kg Gadolinium-DTPA in MS patients only.

All scans, except for the FastPACE sequence, had identical geometric parameters (field of view = 230 mm, matrix = 256 × 256, slices thickness = 5 mm, slice gap = 0.5 mm, number of slices = 20). The FastPACE sequence used a matrix of 128 × 128 and generated 16 slices, which were positioned to match exactly the central 16 slices of the conventional imaging experiments.

Generation of Quantitative Images

Images showing MTR, k_{for}, and $T1_{free}$ were calculated pixel-by-pixel from the FastPACE data set as described previously (14, 15). In short, $T1_{sat}$ was calculated from two phase images that were acquired with two phase alternated measurements under MT saturation. MTR images were derived from two magnitude images acquired with and without the MT saturation pulse according to the following equation: MTR = (1-M_S/M_0) × 100%, where M_s is the signal intensity in the magnitude image acquired with MT saturation and M_0 the signal intensity without MT saturation. Images showing the transfer rate k_{for} were obtained from the $T1_{sat}$ and MTR images with the formula: $k_{for} = MTR/T1_{sat}$. Finally, $T1_{free}$ images were calculated according to the equation: $T1_{free} = 1/(1/T1_{sat}\text{-}k_{for})$.

All images were calculated on an UltraSPARC 1 workstation (Sun Microsystems, Palo Alto, CA), which was connected by ethernet to the scanner host computer, using home developed software. For further image analysis, only the MTR, k_{for}, and $T1_{free}$ images were used.

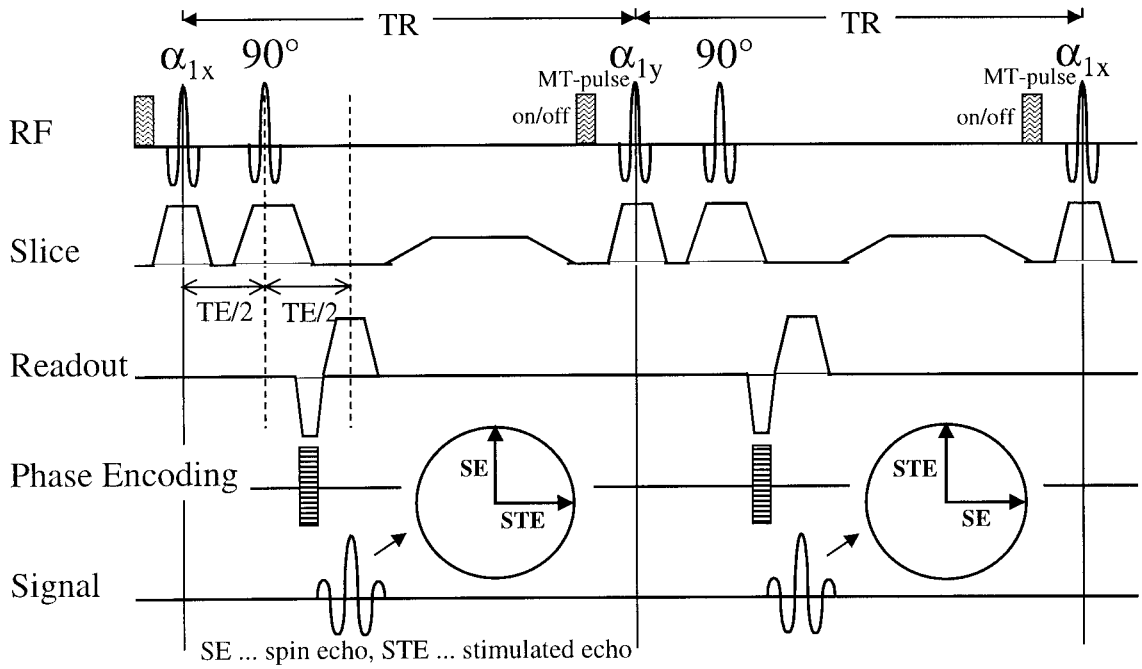

FIG 1. The FastPACE sequence, as used for quantitative magnetization transfer imaging. Two phase-alternated acquisitions for a single phase-encoding step are shown. These two acquisitions are necessary to remove the background phase, because T1 is obtained from the phase of the composite echo. Each TR interval can be exploited for excitation of additional slices. MT saturation is achieved by performing a short binomial pulse before α_1. Owing to multislice acquisition, a high saturation level can be achieved.

Image Analysis

In MS patients, we investigated the following tissue categories as shown by conventional MR imaging: normal-appearing white matter (NAWM), diffuse white matter changes, and focal non-acute and acute lesions. Diffuse white matter changes comprised areas with a subtle, diffuse increase of white matter signal intensity on proton density–weighted images, which may be seen remote from focal lesions and have also been termed ''dirty'' white matter (1). Focal non-acute lesions were subdivided according to their hypointensity on T1-weighted images as isointense and mildly and markedly hypointense. Marked T1 hypointensity corresponded to a signal intensity that was equal to or lower than the gray matter on T1-weighted scans. Acute lesions were subdivided into densely enhancing lesions and ring-enhancing lesions. Areas of marked hyperintensity around enhancing lesions, which disappeared on follow-up scans, were considered to reflect edema.

All lesions visible on the proton density–weighted images were first marked on hardcopy (F. F.). Using these hardcopies as a reference, irregular regions were drawn on the proton density–weighted images and copied to the MTR, k_{for}, and $T1_{free}$ maps by using ANALYZE (Mayo Clinic, Rochester, MN) (S.R.). Only regions larger than 10 mm^2 were selected for further analysis.

The reference values for normal white matter (NWM) from healthy control subjects were obtained by measurements in eight different locations (bilaterally in the frontal and occipital white matter, in the centrum semiovale, and periventricular white matter). The same regions were selected for examination of the NAWM in MS patients, with great care taken to avoid regions that showed diffuse signal changes or were located in the vicinity of focal lesions.

Statistical Analysis

For statistical analysis, we used Statistica software (StatSoft, Tulsa, OK). Comparison of quantitative measures between different groups of white matter and lesion types was performed using the Mann-Whitney *U* test.

Results

Control White Matter

The volunteers' brains were free from signal abnormalities on proton density–weighted and T1-weighted images; therefore, the white matter was considered NWM. In a total of 64 regions of interest, the mean MTR of NWM was 48.7 (±1.2) %, the mean transfer rate k_{for} was 1.43 (±0.10) s^{-1} and the mean $T1_{free}$ was 670 (±51) ms.

Lesion Appearance in MS

All lesions visible on the proton density–weighted images were also visible on the MTR, k_{for}, and $T1_{free}$ images. Although some lesions were hard to differentiate from NAWM on the $T1_{free}$ images, all lesions could be well differentiated from NAWM on the MTR and k_{for} images. Some lesion types such as edema and dirty white matter were separated best from NAWM on k_{for} images. A respective example comparing the appearance of subtle white matter changes on proton density–weighted, T1-weighted, and k_{for} images is given in Figure 2.

Quantitative MT Values in MS

We analyzed a total of 296 white matter areas. They comprised 72 regions of NAWM, six regions of dirty white matter, and 218 focal MS lesions. The majority of focal lesions was non-acute, with 75 isointense and 79 mildly and 43 markedly hypointense on T1-weighted scans. Among the acute lesions, 10 were densely enhancing, eight showed

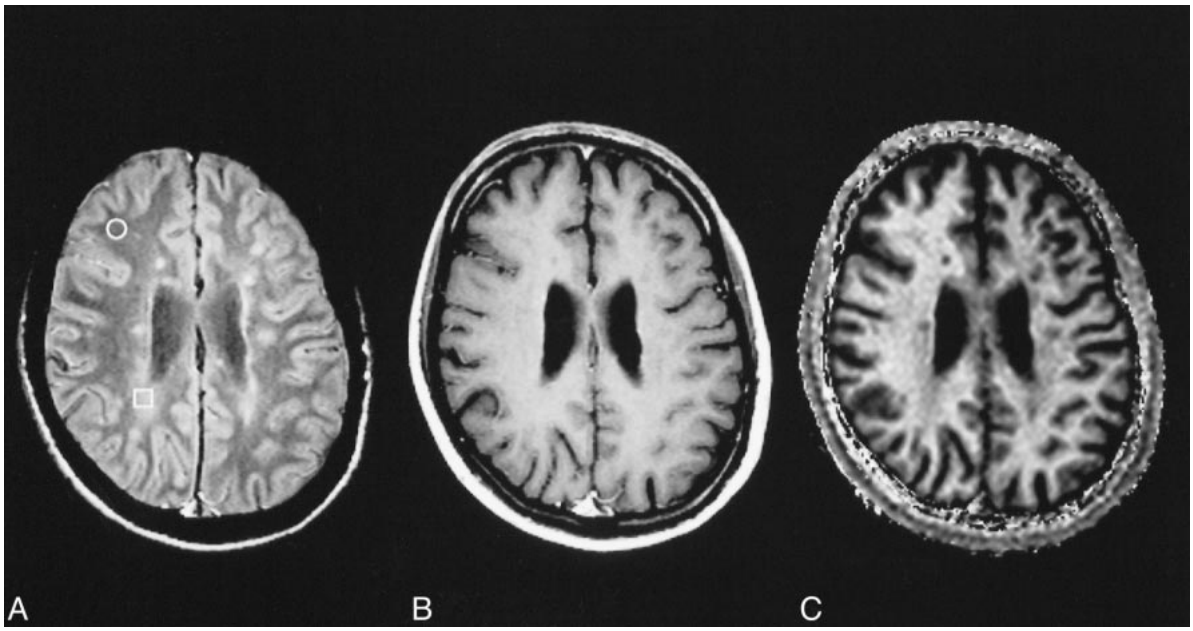

FIG 2. NAWM (*circle*) and "dirty white matter" (*square*) in MS on spin-echo proton density–weighted (2060/20/1) image (*A*). No corresponding changes are seen on the postcontrast T1-weighted (510/14/2) image (*B*). In the calculated image showing the transfer rate k_{for}, the area of dirty white matter is clearly visible (*C*).

Mean values and SD of MTR, k_{for}, and T_{free} for NWM, NAWM, and different lesion types

	Type	N	MTR [%] Mean (SD)	$T1_{free}$ [ms] Mean (SD)	k_{for} [sec^{-1}] Mean (SD)
Control subjects	NWM	64	48.7 (1.2)	670 (51)	1.43 (0.10)
MS patients	NAWM	72	46.6 (1.8)	664 (49)	1.32 (0.10)
Diffuse changes	dirty WM	6	46.2 (2.2)	721 (29)	1.19 (0.09)
Focal lesions					
Non-active	T1 isointensity	75	37.5 (3.6)	803 (68)	0.76 (0.12)
	Mild T1 hypointensity	79	33.1 (4.3)	910 (71)	0.55 (0.11)
	Marked T1 hypointensity	43	25.9 (6.8)	1,159 (168)	0.32 (0.11)
Active	Dense enhancement	10	35.2 (3.5)	822 (30)	0.66 (0.11)
	Ring enhancement	8	25.2 (4.1)	1,048 (237)	0.34 (0.11)
	Edema	3	39.2 (2.6)	1,250 (20)	0.51 (0.06)

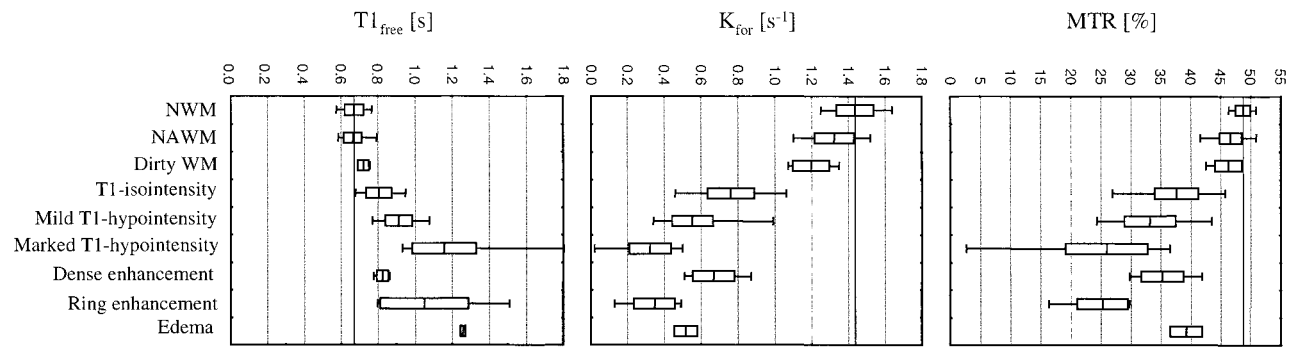

FIG 3. MTR, k_{for}, and $T1_{free}$ of different lesion types. The whiskers represent the range, the box represents the SD, and the line indicates the mean value. The mean value for NWM is marked by the solid line across the graph.

ringlike enhancement, and three were surrounded by edema. Quantitative results obtained in these different white matter conditions of MS patients are summarized in the Table and illustrated in Figure 3.

The MTR of both NAWM and dirty white matter of MS patients was significantly reduced when compared with the MTR of control NWM ($P < .001$). However, there was no difference in the

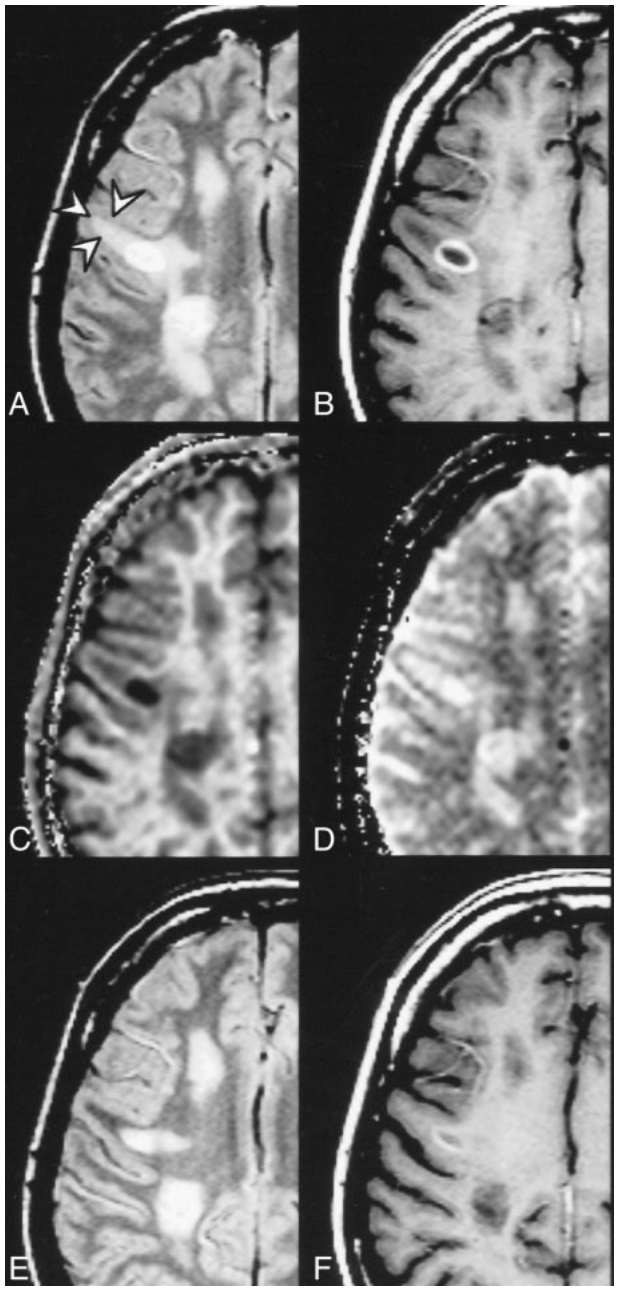

FIG 4. Ring-enhancing lesion surrounded by edema (*arrows*) and multiple non-active lesions. Proton density–weighted (2060/20/1) (*A*), postcontrast T1-weighted (510/14/2) (*B*), k_{for} (*C*), and $T1_{free}$ (*D*) images. The quantitative analysis in the acute lesions yielded the following results: ring-enhancing lesion: MTR = 16.4 %, k_{for} = 0.13 s^{-1}, $T1_{free}$ = 1.5 s; edema: MTR = 41.1 %, k_{for} = 0.56 s^{-1}, $T1_{free}$ = 1.2 s. Proton density–weighted (*E*) and postcontrast T1-weighted (*F*) images acquired 6 weeks later. Disappearance of perifocal signal abnormality supports the assumption of edema.

MTR between NAWM and dirty white matter. Although the transfer rate was also significantly lower in NAWM ($P < .001$) and in dirty white matter ($P = .022$) compared with NWM, there was no difference between $T1_{free}$ of NAWM and NWM. However, $T1_{free}$ of dirty white matter was found to be significantly increased ($P = .012$).

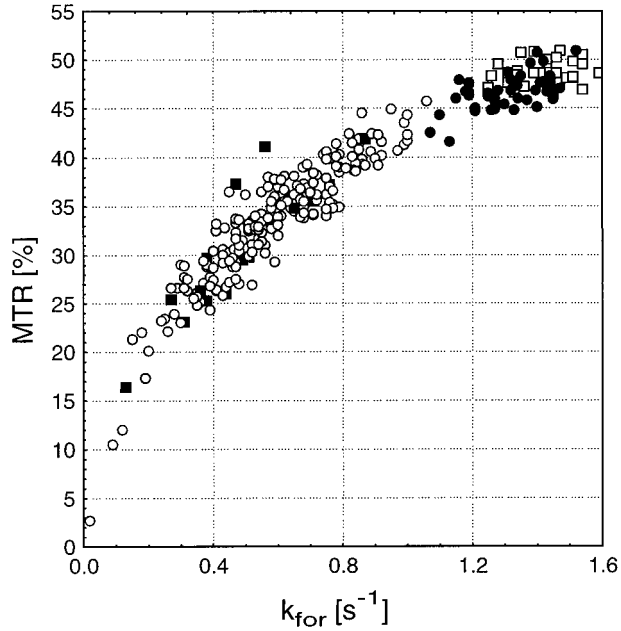

FIG 5. MTR versus k_{for} for different lesion types. The *open squares* show NWM. The *filled circles* show areas with diffuse changes. Non- active lesions are represented by the *open circles,* and active lesions are represented by the *filled squares.* The clustered groups show a good correlation between MTR and k_{for}; however, the overall relationship is non-linear.

Focal non-active lesions showed a gradual decline of MTR and k_{for} values with greater T1 hypointensity. Inversely, $T1_{free}$ was noted to increase with T_1 hypointensity. Different and more complex patterns were seen within active lesions. The MTR was lowest in ring-enhancing lesions and highest in edema. K_{for} was lowest in ring-enhancing lesions but highest in densely enhancing lesions. $T1_{free}$ was lowest in densely enhancing lesions and highest in edema. A representative set of proton density–weighted, T1-weighted, and quantitative images of a ring-enhancing lesion with edema is given in Figure 4.

Overall, the pattern of k_{for} value distribution correlated very well with changes in MTR when excluding edema and dirty white matter from such consideration. However, this correlation was nonlinear, as shown in Figure 5, which suggests a different range of information that is provided by k_{for} and MTR on non-active lesions of MS.

Discussion

MT imaging is a powerful method for tissue analysis by characterizing the interaction of free water protons with the pool of protons bound to macromolecules. Previous work in MS has used the MTR as a semiquantitative measure of the MT effect to describe focal and diffuse white matter damage (24). Using the FastPACE sequence, we attempted to provide complementary information by obtaining estimates on two variables, k_{for} and $T1_{free}$, which contribute to the MTR.

Part of the interest in MTR measurements for investigating MS pathologic abnormalities is based on speculations that the MTR of white matter is largely determined by myelin content (25). This is supported by a reduction of the MTR that parallels the severity of white matter destruction seen histopathologically (26). The magnetization transfer rate k_{for} describes the intensity of interaction between the free water protons and myelin to exchange magnetization. This process is thought to take place primarily at the site of macromolecules containing polar groups such as cholesterol (7, 27) and would also be expected to diminish with loss of myelin. Consequently, our finding of a close correlation between k_{for} and the MTR across different types of MS lesions lends further support to the validity of using MTR as a measure of white matter integrity. The non-linearity of this relation may suggest a different sensitivity of these variables for MT-related changes at different stages or types of tissue destruction, but could at least partially also be a consequence of differences in the scaling of MTR and k_{for}.

Our findings suggest that further variables affecting the MTR such as the relative contribution of free water expressed by $T1_{free}$ should also be considered in MT analyses. It is still debated, for example, what pathologic abnormalities cause the reduction of MTR in the NAWM of MS patients, which we also observed in our study group (28, 29). It has been speculated that a slight decrease of the MTR could stem from a somewhat higher water content of the NAWM, such as that caused by subtle disruption of the blood-brain barrier (29). On the other hand, demyelination and even axonal loss have been described in histopathologic examinations of NAWM (30, 31), and still others have incriminated the presence of minute inflammatory foci (32). Our finding of normal $T1_{free}$ in NAWM clearly argues against the presence of diffuse edema. However, in regions of mildly increased white matter signal intensity, ie, so-called dirty white matter, $T1_{free}$ measurements suggested a significant increase in water content in addition to damaged myelin. Interestingly, such regions also appear to have a higher probability for newly developing focal lesions (33), which could be the consequence of a more permeable blood-brain barrier.

Quantitation of k_{for} and $T1_{free}$ showed quite profound differences among acute lesions. Densely enhancing lesions had a rather low water content compared with ring-enhancing lesions. This confirms the variability of MS lesion formation (5). How these differences relate to lesion severity, including the grade of involvement of different tissue elements, and translate into subsequent permanent tissue damage will have to be resolved by follow-up studies.

Analyzing different MT variables also appears useful for determining the contribution of edema. It has been repeatedly suggested that edema without demyelination leads to only moderate MTR reduction (8, 9, 34, 35). This is in line with our observations. However, a moderate reduction of the MTR may be also found with both demyelination and increased water content, as was evident in T1-isointense non-acute lesions from the combination of a slightly reduced magnetization transfer rate in parallel with a high $T1_{free}$. Considering different types of focal non-acute lesions, we found a decrease of the MTR and of the transfer rate k_{for} and an increase in water content, which paralleled the extent of hypointensity as seen on T1-weighted scans. This is highly consistent with correlative MR imaging—histopathologic studies that substantiated a close association between the severity of tissue destruction and T1 hypointensity (36–38).

In the interpretations of our results, several methodologic issues should be considered. These are primarily centered on the validity of the two-pool model for describing MT mechanisms in vivo and on the presumed dependence of derived parameters on the experimental condition. The magnetization rate, k_{for}, and the relative contribution of free water, $T1_{free}$, should therefore be considered as estimates despite reassuring methodologic data for our approach (14). Nevertheless, these first results already demonstrate their potential for a further discrimination of MT mechanisms to improve the analysis and understanding of MS-related tissue changes.

References

1. Fazekas F, Barkhof F, Filippi M, et al. **The contribution of magnetic resonance imaging to the diagnosis of multiple sclerosis.** *Neurology* 1999;53:448–456
2. Miller DH, Albert PS, Barkhof F, et al. **Guidelines for the use of magnetic resonance techniques in monitoring the treatment of multiple sclerosis.** *Ann Neurol* 1996;39:6–16
3. Miller DH, Grossman RI, Reingold SC, McFarland HF. **The role of magnetic resonance techniques in understanding and managing multiple sclerosis.** *Brain* 1998;121:3–24
4. Balaban RS, Ceckler TL. **Magnetization transfer contrast in magnetic resonance imaging.** *Magn Reson Q* 1992;8:116–137
5. Lassmann H. **Neuropathology in multiple sclerosis: new concepts.** *Mult Scler* 1998;4:93–98
6. Koenig SH, Brown RD, Spiller M, Lundbom N. **Relaxometry of brain: why white matter appears bright in MRI.** *Magn Reson Med* 1990;14:482–495
7. Fralix TA, Ceckler TL, Wolff SD, Simon SA, Balaban RS. **Lipid bilayer and water proton magnetization transfer: effect of cholesterol.** *Magn Reson Med* 1991;18:214–223
8. Dousset V, Grossman RI, Ramer KN, et al. **Experimental allergic encephalomyelitis and multiple sclerosis: lesion characterization with magnetization transfer imaging.** *Radiology* 1992;182:483–491
9. Mehta RC, Pike B, Enzmann DR. **Measure of magnetization transfer in multiple sclerosis demyelinating plaques, white matter ischemic lesions, and edema.** *AJNR Am J Neuroradiol* 1996;17:1051–1055
10. Gass A, Barker GJ, Kidd D, et al. **Correlation of magnetization transfer ratio with clinical disability in multiple sclerosis.** *Ann Neurol* 1994;36:62–67
11. Buchem MA, Grossman RI, Armstrong C, et al. **Correlation of volumetric magnetization transfer imaging with clinical data in MS.** *Neurology* 1998;50:1609–1617
12. Henkelman RM, Huang X, Xiang QS, Stanisz GJ, Swanson SD, Bronskill MJ. **Quantitative interpretation of magnetization transfer.** *Magn Reson Med* 1993;29:759–766
13. Wolff SD, Balaban RS. **Magnetization transfer contrast (MTC) and tissue water proton relaxation in vivo.** *Magn Reson Med* 1989;10:135–144

14. Ropele S, Stollberger R, Hartung HP, Fazekas F. **Estimation of magnetization transfer rates from PACE Experiments with pulsed RF saturation.** *J Magn Reson Imaging,* In press
15. Ropele S, Stollberger R, Hartung HP, Toyka K, Fazekas F. **Quantitative magnetization transfer imaging in human brain by means of a PACE technique.** Proceeding of ISMRM Seventh Scientific Meeting, Philadelphia, 1999;1917
16. Ropele S, Stollberger R, Kapeller P, Hartung HP, Fazekas F. **Fast multislice T_1 and T_{1sat} imaging using a PACE technique.** *Magn Reson Med* 1999;42:1089–1097
17. Edzes HT, Samulski ET. **Cross relaxation and spin diffusion in the proton NMR of hydrated collagen.** *Nature* 1977;265:512–523
18. Hu BS, Conolly SM, Wright GA, Nishimura DG, Macovksi A. **Pulsed saturation transfer contrast.** *Magn Reson Med* 1992;26: 231–240
19. Koenig SH, Brown RD. **The importance of motion of water for magnetic resonance imaging.** *Invest Radiol* 1985;20:297–305
20. Forsen S, Hoffman A. **Study of moderately rapid chemical exchange reactions by means of nuclear magnetic double resonance.** *J Chem Phys* 1963;39:2892–2901
21. Yeung HN. **On the treatment of the transient response of a heterogeneous spin system to selective RF saturation.** *Magn Reson Med* 1993;30:146–147
22. Graham SJ, Henkelman RM. **Understanding pulsed magnetization transfer.** *J Magn Reson Imaging* 1997;7:903–912
23. Kurtzke JF. **Rating neurological impairment in multiple sclerosis: an expanded disability status scale (EDSS).** *Neurology* 1983;33:1444–1452
24. Filippi M, Grossman R, Comi G. **Magnetization transfer imaging in multiple sclerosis.** *Neurology* 1999[3]:53
25. Stanisz GJ, Kecojevic A, Bronskill MJ, Henkelman RM. **Characterizing white matter with magnetization transfer and T_2.** *Magn Reson Med* 1999;42:1128–1136
26. van Waesberghe JH, Kamphorst W, De Groot CJ, et al. **Axonal loss in multiple sclerosis lesions: magnetic resonance imaging insights into substrates of disability.** *Ann Neurol* 1999;46:747–754
27. Kucharczyk W, Macdonald PM, Stanisz GJ, Henkelman RM. **Relaxivity and magnetization transfer of white matter lipids at MR imaging: importance of cerebrosides and pH.** *Radiology* 1994;192:521–529
28. Loevner LA, Grossman RI, Cohen JA, Lexa FJ, Kessler D, Kolson DL. **Microscopic disease in normal-appearing white matter on conventional MR images in patients with multiple sclerosis: assessment with magnetization-transfer measurements.** *Radiology* 1995;196:511–515
29. Filippi M, Rocca MA, Martino G, Horsfield MA, Comi G. **Magnetization transfer changes in the normal appearing white matter precede in the appearance of enhancing lesions in patients with multiple sclerosis.** *Ann Neurol* 1998;43:809–814
30. Fu L, Matthews PM, De Stefano N, et al. **Imaging axonal damage of normal-appearing white matter in multiple sclerosis.** *Brain* 1998;121:103–113
31. Trapp BD, Peterson J, Ransohoff RM, Rudick R; Mörk S, Bö L. **Axonal transection in the lesions of multiple sclerosis.** *N Engl J Med* 1998;338:278–285
32. Cercignani M, Iannucci G, Rocca MA, Comi G, Horsfield MA, Filippi M. **Pathologic damage in MS assessed by diffusion-weighted and magnetization transfer MRI.** *Neurology* 2000;54: 1139–1144
33. Zhao GJ, Li DK, Cheng Y, Wang XY, Paty DW and the UBC MS/MRI research group. **Active multiple sclerosis lesions occur in dirty-appearing white matter as detected by serial magnetic resonance imaging.** *Ann Neurol* 1998;44:465
34. Lai HM, Davie CA, Gass A, et al. **Serial magnetization transfer ratios in gadolinium-enhancing lesions in multiple sclerosis.** *J Neurol* 1997;244:308–311
35. Kimura H, Grossman RI, Lenkinski RE, Gonzalez-Scarano F. **Proton MR spectroscopy and magnetization transfer ratio in multiple sclerosis: correlative findings of active versus irreversible plaque disease.** *AJNR Am J Neuroradiol* 1996;17:1539–1547
36. van Walderveen MA, Barkhof F, Hommes OR, et al. **Correlating MRI and clinical disease activity in multiple sclerosis: relevance of hypointense lesions on short TR/short TE ("T1-weighted") spin-echo images.** *Neurology* 1995;45:1684–1690
37. Truyen L, van Waesberghe JH, van Walderveen MA, et al. **Accumulation of hypointense lesions ("black holes") on T1 SE MRI in multiple sclerosis correlates with disease progression.** *Neurology* 1996;47:1469–1476
38. van Walderveen MA, Kamphorst W, Scheltens P, et al. **Histopathologic correlate of hypointense lesions on T1-weighted spin-echo MRI in multiple sclerosis.** *Neurology* 1998;50:;1282–1288